

# Quantum metasurfaces as probes of vacuum particle content

Germain Tobar,<sup>1</sup> Joshua Foo,<sup>2</sup> Sofia Qvarfort,<sup>1,3</sup> Fabio Costa,<sup>3</sup> Rivka Bekenstein,<sup>4</sup> and Magdalena Zych<sup>1</sup>

<sup>1</sup>*Department of Physics, Stockholm University, SE-106 91 Stockholm, Sweden*

<sup>2</sup>*Department of Physics and Astronomy, University of Waterloo, Waterloo, Ontario, Canada, N2L 3G1*

<sup>3</sup>*Nordita, KTH Royal Institute of Technology and Stockholm University,  
Hannes Alfvens väg 12, SE-114 19 Stockholm, Sweden*

<sup>4</sup>*Racah Institute of Physics, The Hebrew University of Jerusalem, Jerusalem 91904, Israel*

(Dated: March 7, 2025)

The quantum vacuum of the electromagnetic field is inherently entangled across distinct spatial sub-regions, resulting in non-trivial particle content across these sub-regions. However, accessing this particle-content in a controlled laboratory experiment has remained far out of experimental reach. Here we propose to overcome this challenge with a quantum mirror made from a two-dimensional sub-wavelength array of atoms that divides a photonic cavity. The array's response to light is tunable between transmissive and reflective states by a control atom that is excited to a Rydberg state. We find that photon content from entangled sub-regions of the vacuum causes frequency shifts that are accessible to existing experimental setups. This feasibility stems from the system's unique ability to create coherent superpositions of transmissive and reflective states, providing the first practical platform for directly observing particle content from entangled spatial sub-regions of the electromagnetic field vacuum.

## I. INTRODUCTION

In any relativistic quantum field theory, including quantum electrodynamics (QED), local regions of the field are not in the vacuum state even when the global field is in the vacuum [1–5]. This is because vacuum states of relativistic field theories contain local fluctuations. The key physical consequence of this phenomenon is the prediction of non-zero particle content in sub-regions of a quantum field that is in its global vacuum state. Various cavity QED experiments have explored the unique properties of the QED vacuum, such as the cooperative Lamb shift observed in atomic ensembles [6, 7]. A significant challenge in modern vacuum QED experiments is detecting particle content from the vacuum, where photons from spatial sub-regions of the vacuum become observable. This phenomenon occurs in a QED system when for example a mirror's motion alters the electromagnetic field vacuum mode profiles, known as the dynamical Casimir effect (DCE) [8–11]. At sufficiently high speeds, vacuum modes fail to adiabatically adjust to the mirror's new position, leading to a mismatch between the updated cavity modes and the original quantum state. This mismatch generates non-trivial particle content, which, if detected, would correspond to photons spontaneously produced from entangled spatial sub-regions of the vacuum.

The experimental observation of this phenomenon is a key objective for experiments at the interface of relativity and quantum theory because particle creation from the vacuum is also closely related to several fundamental yet unobserved phenomena such as Unruh and Hawking radiation [12–15], and bridges several disciplines including quantum optics [16] and quantum field theory in curved spacetime [17, 18], with applications to analogue gravity [19–21]. In this way, unambiguous confirmation of the local particle content of distinct spatial sub-regions of the vacuum, would mark a major milestone in experiments in relativistic quantum physics.

The practicality of observing vacuum particle creation with a physical mirror has been debated, since a macroscopic ob-

ject moving at the required relativistic speeds would endure immense mechanical stress, making the experiment highly impractical, with arguments being raised that it might be fundamentally impossible [22]. Seminal experiments have successfully demonstrated particle creation from the vacuum without moving a mirror, instead generating observable photons by modulating the electric boundary conditions of a superconducting cavity [23] or using light in a superconducting metamaterial [24]. However, these experiments rely on resonant enhancement to produce the time-dependent boundary conditions in the DCE, where a single quantum of a driving field is converted into two entangled photons via a parametric process. Furthermore, since the electromagnetic mode boundary conditions change only perturbatively, such experiments cannot be interpreted as observing particle content of distinct entangled spatial sub-regions of the vacuum. In contrast, the authors of Ref. [25] proposed to use a rapidly slammed mirror in a photonic cavity to generate local particles of spatial sub-regions of the vacuum. However, this has remained far out of experimental reach due to the extremely high speed at which the mirror needs to be inserted in the cavity.

In parallel, atomic arrays are at the forefront of modern quantum physics, with transformative applications in quantum computing, quantum simulation, quantum sensing and metrology [26–32], most recently as superradiant sensors for the Unruh effect [33, 34]. Their applicability in cavity set-ups is also receiving more attention, notably for their ability to provide confining mirrors in a cavity set-up [35]. In addition, they have been proposed as platforms for realising a quantum metasurface [36], in which the atomic array can be toggled between superpositions of transmissive ( $|T\rangle$ ) and reflective ( $|R\rangle$ ) states via control of the internal state of a single atom.

In this article, we propose a protocol to measure the local particle content of entangled spatial sub-regions of the electromagnetic vacuum using a quantum metasurface—realised as a two-dimensional sub-wavelength atomic array [36]—that divides a photonic cavity. Vacuum particle creation induces a

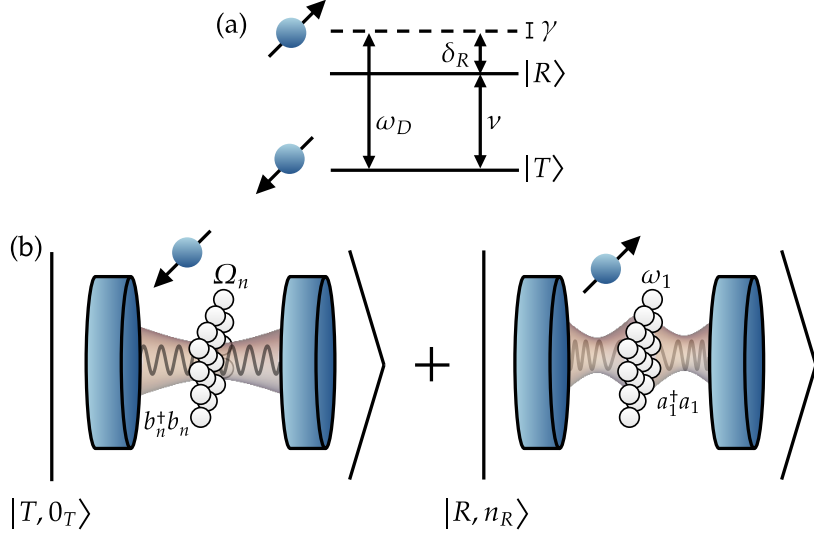


FIG. 1: a) The presence of particle creation from the vacuum due to a change in the atom array's reflectivity produces a frequency shift  $\delta_R$  of the transition frequency  $\nu$  of the control atom for the two-dimensional atomic array when the control atom is driven with drive frequency  $\omega_D$ . The frequency shift is much larger than the atomic line-width  $\gamma$  of the ancilla atom. b) A quantum metasurface acts as a quantum-controlled mirror within a photonic cavity, where superpositions of reflective ( $|R\rangle$ ) and transmissive ( $|T\rangle$ ) states are induced by driving the control Rydberg atom. This quantum superposition dynamically induces superpositions of the electromagnetic cavity's boundary conditions, leading to observable frequency shifts of the control atom. These effects serve as a witness of particle content from entangled spatial sub-regions of the electromagnetic field vacuum, achievable without the need for classical rapid mirror motion.

measurable frequency shift in the control atom of the atomic array, a shift that is eight orders of magnitude larger than the atomic line-width. This signature is detectable through measurements of the photonic cavity's power spectrum, placing it within reach of current experimental capabilities. This removes the need for rapid modulation of a classical mirror's reflectivity to observe vacuum particle creation and, moreover, enables new experiments probing local particle content in the vacuum by generating coherent superpositions of distinct QED vacua. Definitive observation of this particle content would correspond to the first experimental signature of the entanglement structure of the quantum vacuum.

## II. SUB-REGION PARTICLE CONTENT WITH A CLASSICAL MIRROR

We begin by outlining the theoretical framework for observing photon content from entangled spatial sub-regions of the vacuum with a rapidly introduced mirror, examined in Ref. [25]. Consider a photonic cavity of length  $L$ , where the mode functions satisfying the Klein-Gordon equation with Dirichlet boundary conditions are given by [25]:

$$U_n(x, t) = \frac{1}{\sqrt{L\Omega_n}} \sin\left(\frac{\pi n x}{L}\right) e^{-i\Omega_n t}, \quad (1)$$

where  $\Omega_n = \frac{\pi n c}{L}$  are the resonance frequencies of the photonic cavity. The corresponding eigenstates are Fock states

of the cavity's free Hamiltonian,  $\hat{H} = \sum_{n=1}^{\infty} \Omega_n \hat{b}_n^\dagger \hat{b}_n$ , where  $\hat{b}_n^\dagger$  and  $\hat{b}_n$  are creation and annihilation operators for mode  $n$ , satisfying commutation relations  $[\hat{b}_n, \hat{b}_m^\dagger] = \delta_{nm}$ . Now, if a mirror is suddenly introduced at time  $t = 0$  within the cavity, it alters the boundary conditions and introduces time-dependence into the Hamiltonian [25]:

$$\hat{H}(t) = \begin{cases} \sum_n \Omega_n \hat{b}_n^\dagger \hat{b}_n & t < 0 \\ \sum_m \omega_m \hat{a}_m^\dagger \hat{a}_m + \bar{\omega}_m \hat{\bar{a}}_m^\dagger \hat{\bar{a}}_m & t \geq 0, \end{cases} \quad (2)$$

where  $\omega_m = \frac{\pi m}{r}$ ,  $\bar{\omega}_m = \frac{\pi m}{\bar{r}}$  are the frequencies of the left and right sub-cavities of length  $r$  and  $\bar{r} = L - r$  respectively. This sudden change implies the physics of the resulting sub-cavities is better described through the Bogoliubov relation between  $\hat{b}_n$  and the sub-cavity modes  $\hat{a}_j, \hat{\bar{a}}_j$  [25]. In particular, the mode transformation for  $\hat{a}_j, \hat{\bar{a}}_j$  take the form:

$$\begin{aligned} \hat{a}_j &= \sum_{n=1}^{\infty} \left( \alpha_{jn} \hat{b}_n - \beta_{jn} \hat{b}_n^\dagger \right) \\ \hat{\bar{a}}_j &= \sum_{n=1}^{\infty} \left( \bar{\alpha}_{jn} \hat{b}_n - \bar{\beta}_{jn} \hat{b}_n^\dagger \right), \end{aligned} \quad (3)$$

here the Bogoliubov coefficients are  $\alpha_{jn} = \frac{j(-1)^j}{\sqrt{n}j a \pi (n - \frac{j}{a})} \sin(n\pi a)$  and  $\beta_{jn} = \frac{j(-1)^j}{\sqrt{n}j a \pi (n + \frac{j}{a})} \sin(n\pi a)$  for the left sub-cavity, and  $\bar{\alpha}_{jn} = \frac{-j}{\sqrt{n}j \bar{a} \pi (n - \frac{j}{\bar{a}})} \sin(n\pi a)$  and  $\bar{\beta}_{jn} = \frac{-j}{\sqrt{n}j \bar{a} \pi (n + \frac{j}{\bar{a}})} \sin(n\pi a)$  for the right sub-cavity (where

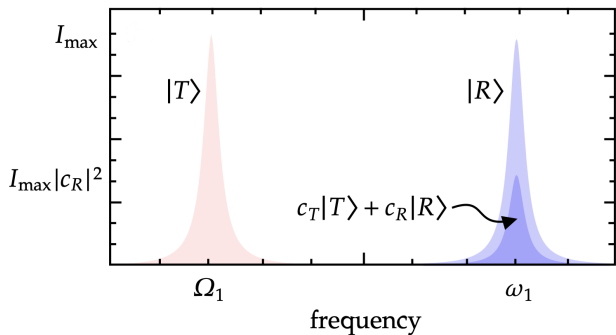


FIG. 2: The average field intensity in the cavity over multiple measurements is weighted by the amplitude,  $c_R$  or  $c_T$ , of the mirror to be in its reflective ( $|R\rangle$ ), or transmissive ( $|T\rangle$ ), state. If the control atom is initialised in its ground state, only when the control atom is driven at the re-normalised transition frequency, due to the presence of sub-region particle content, does the Lorentzian peak at the sub-cavity frequency appear with substantial amplitude.

$a = \frac{r}{L}$ ,  $\bar{a} = \frac{\bar{r}}{L}$  is the ratio between the cavity lengths of the left and right sub-cavities to the global cavity respectively). These Bogoliubov coefficients quantify the mixing between the original modes and the new modes due to the mirror's sudden introduction. The nonzero  $\beta_{jn}, \bar{\beta}_{jn}$  coefficients signify local photon content in the global vacuum, as the vacuum state of the global cavity is no longer empty in terms of the sub-cavity modes.

The average number of sub-cavity photons in mode  $i$ , evaluated in the vacuum state of the original global cavity, is given by  $\langle \hat{n}_i(t) \rangle = \sum_{n \geq 1} |\beta_{in}|^2$ . For the extremal case where the mirror is placed at the midpoint of the cavity, such that the ratio of the sub-cavity length to the global cavity length is  $a = 0.5$ , the number of created photons can reach values as high as  $\langle \hat{n}_i(t) \rangle \approx 0.05$ . However, achieving this effect requires the spatial boundary conditions of the cavity to change non-perturbatively (in contrast to the experiments of Refs. [23, 24]) on a timescale faster than the free evolution of the cavity modes. It was suggested in [25] that a classical mirror with rapidly varying reflectivity could induce such fast and non-perturbative spatial boundary condition changes. Yet, this approach demands changes on the order of  $10^{-14}$  s, which is far beyond current experimental capabilities due to the limitations of material response times [37].

### III. OBSERVING SUB-REGION PARTICLE CONTENT WITH A QUANTUM METASURFACE

In order to observe particle content from the vacuum with a classical metasurface, the transition from a transmissive to reflective metasurface would have to occur rapidly. In contrast, in this section we show how a quantum metasurface can make such particle content observable without the need for rapid response times. In our proposal, a quantum metasurface is bounding a photonic cavity and as a result, the mode pro-

file of the photonic cavity depends on the quantum state of a qubit, which has a transition frequency  $\nu$  between its two orthogonal states. The qubit's states represent different optical responses of a quantum metasurface that can be in a superposition of transmissive ( $|T\rangle$ ) or reflective ( $|R\rangle$ ) states. Ref. [36] demonstrated that a two-dimensional sub-wavelength array of atoms can be tuned into superpositions of transmissive and reflective states when preparing the control qubit state in superposition of Rydberg and ground state. Building on these results, we adapt the approach from [36], where near-unit reflectivity was shown to be experimentally feasible. We further use results from Ref. [35], in which it was shown to be feasible to use sub-wavelength atomic arrays as the end of a photonic cavity for a narrow electromagnetic field frequency range  $\Delta \ll \omega_1$  (where  $\omega_1$  is the frequency of the fundamental mode of the photonic cavity formed) with conventional QED parameters. This implies that the atomic array can feasibly confine a single photonic mode. The Hamiltonian of the cavity, therefore, becomes dependent on this quantum-controlled state,  $\hat{H} = \hat{H}_{\text{cav}} + \hat{H}_{\text{switch}} + \hat{H}_{\text{free}}$ , where

$$\begin{aligned} \hat{H}_{\text{cav}} &= \hat{H}_T \otimes |T\rangle\langle T| + \hat{H}_R \otimes |R\rangle\langle R| \\ \hat{H}_{\text{switch}} &= g(|T\rangle\langle R| e^{i(\omega_D - \nu)t} + \text{h.c.}) \\ \hat{H}_{\text{free}} &= \frac{\hbar\nu}{2} (|R\rangle\langle R| - |T\rangle\langle T|). \end{aligned} \quad (4)$$

Here,  $\hat{H}_T = \sum_n \Omega_n \hat{b}_n^\dagger \hat{b}_n$  is the Hamiltonian conditioned on the control being in the transmissive state.  $\hat{H}_R$  represents the reflective Hamiltonian, which reflects the fundamental subcavity mode (that the array reflects) but leaves the global modes unperturbed,  $\hat{H}_R = \sum_n \Omega_n \hat{b}_n^\dagger \hat{b}_n + \omega_1 \hat{a}_1^\dagger \hat{a}_1$ . This approximation is valid in the regime for which the global cavity length is much larger than the sub-cavity length  $L \gg r$ , and the array is reflective in a narrow frequency range,  $\Delta$ , much smaller than the sub-cavity mode spacing  $\Delta \ll \omega_1$  which we justify in Appendix A. We denote  $g$  to be the coupling strength between the control atom and the external drive. The term  $\hat{H}_{\text{switch}}$  allows for the control atom to drive transitions between the transmissive and reflective cavity states. Although switching the control atom between states takes  $O(g)$  time, in the reflective branch of the superposition, the atom array's reflectivity turns on almost instantly. This happens in about the time it takes for light to travel from the control atom to the array, which—within the Rydberg blockade radius—is much faster than the optical mode's free evolution. This causes the reflective branch of the superposition to contain non-zero particle content with respect to the initial global cavity, which will produce an observable frequency shift ( $\delta_R$ ) of the control atom. We note that the atomic array's reflectivity to a single frequency allows it to simultaneously support standing waves of the global and sub-cavity modes, which is distinct from the perfectly reflective mirror considered in Eq. (2).

The effect of the local particle content of the cavity vacuum can be best understood by considering the form of the free Hamiltonian of the atom and the cavity,  $\hat{H}_{\text{cav}} + \hat{H}_{\text{free}}$ , and considering a weak drive  $g \ll \omega_1$ , where  $\omega_1$  is the frequency

of the fundamental mode of the sub-cavity. This expression can be reorganised to emphasize how the control system's energy levels depend on the metasurface response and thus the modes of the photonic cavity,

$$\hat{H}_{\text{cav}} + \hat{H}_{\text{free}} = \left( \hat{H}_R + \frac{\hbar\nu}{2} \right) \otimes |R\rangle\langle R| + \left( \hat{H}_T - \frac{\hbar\nu}{2} \right) \otimes |T\rangle\langle T|,$$

where it becomes clear that the energy levels of the control atom are renormalised by the distinct energy contributions from the global and sub-cavities, described by  $\hat{H}_T$  and  $\hat{H}_R$  respectively. The frequency shift depicted in Fig. 1 ( $\delta_R$ ) can thus be interpreted as a shift in the atom's resonance frequency, which is caused by the differing energy states of these two cavity regions. As we will discuss further, this shift arises due to the sub-cavity containing non-zero particle content for the global cavity vacuum state.

In order to further understand the frequency shift, we now move to the interaction picture with respect to  $\hat{H}_{\text{cav}} + \hat{H}_{\text{free}}$ , where the unitary evolution of the system, up to first order in  $g$  is

$$\hat{U}_I^{(1)} = \hat{\mathbb{I}} - ig \int_0^t dt' \left( e^{i\hat{H}_R t'} |R\rangle\langle T| e^{-i(\hat{H}_T + \delta)t'} + \text{h.c.} \right), \quad (5)$$

where  $\delta = \nu - \omega_D$  is the detuning between the laser frequency and atomic transition. Starting from an initial vacuum state of the global cavity  $|0_T\rangle$  and the state of the control qubit for which the metasurface is transmissive  $|T\rangle$ , the probability to measure the control atom in the reflective state  $|R\rangle$  becomes:

$$P_R = 4(gt)^2 \left\langle \text{sinc}^2 \left( \frac{1}{2} \left( \delta + \omega_1 \hat{a}_1^\dagger \hat{a}_1 + \sum_n \Omega_n \hat{b}_n^\dagger \hat{b}_n \right) t \right) \right\rangle \approx 4(gt)^2 \left\langle \text{sinc}^2 \left( \frac{1}{2} (\delta + \delta_R) t \right) \right\rangle, \quad (6)$$

where  $\langle \dots \rangle$  is taken with respect to  $|0_T\rangle$ ,  $\hat{a}_1$  and  $\hat{b}_n$  represent the fundamental sub-cavity and global mode operators respectively, and  $\delta_R = \sum_n \omega_1 |\beta_{1,n}|^2$  is an analytical estimate of the frequency shift due to the sub-region particle content (see Appendix C) which forms the core experimental signature of vacuum particle content of this work. We present the derivation of this perturbative expression for the transition probability in Appendix B. It is apparent from Eq. (6), that the presence of photons in the sub-cavity with respect to the global cavity vacuum state,  $\langle 0_T | \hat{a}_1^\dagger \hat{a}_1 | 0_T \rangle = \sum_n |\beta_{1,n}|^2 \neq 0$ , produces a frequency shift of the control atom.

Importantly, the fact that the frequency shift arises due to a non-zero number of photons in the sub-cavity for the global cavity vacuum distinguishes it from other vacuum frequency shifts, such as the Lamb shift, which are independent of particle content of spatial sub-regions [38]. We compute this frequency shift, assuming a fundamental sub-cavity mode frequency on the order of 400 THz normalised to a line-width on the order of 10 MHz. Our results demonstrate that the

shift in the transition frequency is on the order of 2.8% of the total transition frequency, but over 6 orders of magnitude larger than the line-width (due to the Bogoliubov transformation contributing a frequency shift that is approximately 7% of the photonic cavity frequency, see Appendix C for more details). This demonstrates how the quantum-controlled mirror can provide the necessary boundary condition changes for photon creation, thus bringing particle creation due to entangled sub-regions of the vacuum within experimental reach. The numbers used to compute the change in the transition frequency are adapted from a state-of-art experimental system of  $^{87}\text{Rb}$  sub-wavelength atom array that has potential for implementation of our proposed scheme [39], or alternatively with Yb atoms [40]. Specifically, we consider the following energy levels:  $|g\rangle = |5 S_{1/2}, F = 2, m_F = -2\rangle$  as the ground state and  $|e\rangle = |5 P_{3/2}, F = 3, m_F = -3\rangle$  as the excited state, resonating at  $\omega_1/2\pi = 400$  THz. Accessing a fundamental mode of this frequency will require a cavity of order sub-micron length. While such a small cavity will increase the resonance line width by a factor proportional to  $\frac{1}{r}$ , this will not substantially reduce the power spectrum for such small resonators. For lattice spacing  $a \approx 0.2\lambda_1$ , where  $\lambda_1$  is the wavelength of the fundamental sub-cavity mode, (also achievable with Yb atoms), corresponding to 156 nm, the array achieves perfect reflectivity [40], making it reflective to modes near  $\omega_1$ . For sub-cavity line-width  $\kappa \ll \omega_1$ , this frequency would be the only supported mode, allowing the atomic array to serve as one end of a sub-cavity, similar to that proposed in Ref. [35]. We consider the Rydberg control atom to also be a  $^{87}\text{Rb}$  atom, but consider the ground state of the ancilla control to be  $|g'\rangle = |5 S_{1/2}, F = 1, m_F = -1\rangle$ , with Rydberg state  $|r_P\rangle = |44 P_{3/2}, m_J = 3/2\rangle$ , which has a transition at  $\nu/2\pi = 1000$  THz, with achievable Rabi drive strengths of  $g/2\pi \sim 1$  MHz [39], and assuming a line-width on the order of  $\gamma/2\pi \approx 10$  MHz. Therefore, for this arrangement of a two-dimensional atomic array, if the array is  $\frac{\lambda_1}{2} \approx 78$  nm from one end of the cavity producing a sub-cavity frequency  $\omega_1$ , the frequency shift of the control atom will be  $\delta_R \sim$  THz, which is orders of magnitude larger than the linewidth.

*Noise and imperfections.* Two main sources of imperfections are thermal motion of the atomic array, and imperfect reflectivity. Regarding the former, assuming an atomic array that has a collective motional DoF cooled to the quantum ground state, the magnitude of thermal motion of the array will be on the order of its zero-point motion [41]. For atoms in a trap frequency on the order of 10 MHz, this motion is on the order of  $10^{-8}$  m, much smaller than length of the fundamental mode of a 400 THz optical cavity. For the latter, we utilise a toy model in Appendix D to compute the particle content produced by a smoothly switched reflective mirror that divides a Dirichlet cavity. Importantly, as the dominant particle content for the single frequency mirror in the main text is due to the fundamental sub-cavity mode, we can apply the corrections for the imperfect reflectivity for the fundamental sub-cavity mode to the single frequency mirror used in the main text. The switching of the mirror is determined by a one-parameter family of time-dependent profiles,  $\theta(t) = (2/\pi) \tan^{-1}((1 + e^{-\lambda t})/(\lambda))$ . Here  $\lambda$  plays a dual

role, namely how close the end state of the mirror is to perfect reflectivity, and how quickly the mirror is switched on (see Fig. 3(a)). By defining an effective reflectivity,  $r_{\text{eff}} = 1 - \theta(\infty)$ , we find that the particle content of the subcavity modes is only slightly suppressed (see Fig. 3(b)) for experimentally expected reflectivities  $r_{\text{eff}} \sim 0.95$  [36].

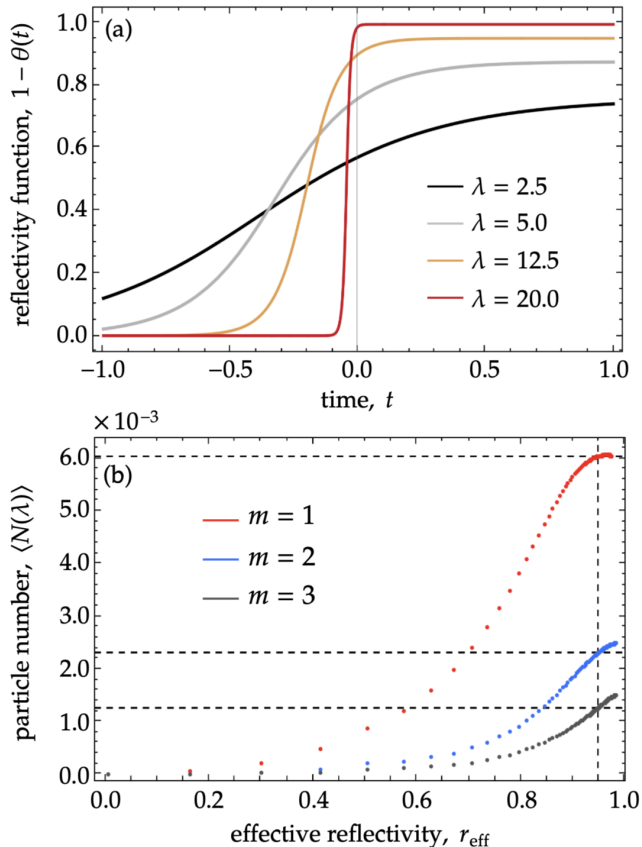


FIG. 3: (a) Plot of the switching profile  $r(t) = 1 - \theta(t)$  as a function of time, where  $r = 1$  corresponds to perfect reflection. The orange curve depicts an effective reflectivity  $r_{\text{eff}} = 0.95$ . (b) Plot of the particle content of the  $m$ -th subcavity mode in the global vacuum state as a function of the effective reflectivity  $r_{\text{eff}}$ . We have plotted this difference for a cavity with walls at  $x = \pm a/2$  with  $a = 1$ . The dashed lines correspond to  $r_{\text{eff}} = 0.95$ . Here,  $\lambda$  serves a dual purpose: it determines both the proximity of the mirror's final state to perfect reflectivity and the speed at which the mirror is activated.

*Proposed Protocol.* The following protocol can be used to verify the predicted vacuum-induced frequency shift of the control atom. Firstly, the control atom is prepared in the ground, and therefore, the transmissive state  $|T\rangle$ . Next, the cavity is pumped on-resonance with the atom's unrenormalised transition frequency  $\nu$ . In this case, due to the frequency shift from the presence of vacuum-photons, there will be a significantly reduced probability for the control atom to flip to the reflective state, as simulated in Appendix E. If the sub-cavity is then pumped on-resonance with sub-cavity mode  $\hat{a}_1$ , the typical Lorentzian peak in the power spectrum

of the output mode (at the frequency  $\omega_1$  of the mode  $\hat{a}_1$ ) will not be observed. Alternatively, if the sub-cavity is pumped on-resonance with the re-normalised transition frequency  $\nu'$ , the array will flip to the reflective state, and the output power spectrum will have a peak at  $\omega_1$  as expected given that the reflective Hamiltonian  $\hat{H}_R$  forms standing waves at the frequency  $\omega_1$ , as illustrated in Fig. 2. This average intensity will be suppressed by  $g^2/\Delta^2$  for a drive detuned from the transition frequency by  $\Delta$ , as demonstrated in Appendix E (the average reflected number of photons will be weighted by the probability for the array to be in the reflective state). For a drive detuned by  $\delta \sim 10^8$  Hz, and coupling strengths as weak as  $g = 10^{-4} \omega_1$ , the suppression of the average intensity is by a factor of  $10^{-5}$  (see Appendix E), compared to the intensity in the sub-cavity on-resonance. Alternatively, if the set-up enables direct access to measurements of the control atom, this frequency shift can be discerned through such direct measurements on the control atom.

#### IV. DISCUSSION

While the particle creation phenomenon predicted in this work shares similarities with previous observations of the dynamical Casimir effect (DCE), it includes crucial differences that allow it to serve as an observation of particle content due to entangled spatial sub-regions of the vacuum. The DCE was originally proposed by Moore as particle production resulting from a moving mirror at the boundary of a one-dimensional photonic cavity [8]. However, for such particle creation to occur at detectable levels, the mirror's motion would need to be relativistic, placing the effect far beyond the reach of realistic experiments. This challenge was later circumvented by leveraging a resonant enhancement through a parametric process [42–44], this resonant enhancement forming the basis of how breakthrough experiments successfully observed the DCE [23, 24]. Despite these advances, these experiments did not investigate particle creation arising from entanglement between distinct spatial sub-regions of the vacuum, as proposed in Ref. [25]. Instead, the observed DCE corresponds to a parametric coupling between pairs of cavity modes induced by the mirror's motion, with boundary conditions only perturbatively modifying the photonic mode profiles. In contrast, the particle creation described in Ref. [25] is fundamentally distinct. It corresponds to detecting photon content associated with entangled, spatially distinct regions of the vacuum state of the electromagnetic field.

In this way, the experimental implementation of our proposal would not only mark the first observation of particle content due to spatial sub-regions of the vacuum, but also serve as the first experimental signature of the entanglement structure of the vacuum.

#### ACKNOWLEDGEMENTS

We thank the participants of the Swedish workshop on analogue gravity, as well as Navdeep Arya, Robert Mann, and

Igor Pikovski for discussions. This material is based upon work supported by the Knut and Alice Wallenberg foundation through a Wallenberg Academy Fellowship No. 2021.0119, and the General Sir John Monash Foundation. J.F. acknowledges funding provided by the National Sciences and Engineering Research Council of Canada through a Banting Post-

doctoral Fellowship. SQ is funded in part by the Wallenberg Initiative on Networks and Quantum Information (WINQ) and in part by the Marie Skłodowska–Curie Action IF programme *Nonlinear optomechanics for verification, utility, and sensing* (NOVUS) – Grant-Number 101027183. Nordita is supported in part by NordForsk.

- 
- [1] H. Reeh and S. Schlieder, Bemerkungen zur unitäräquivalenz von lorentzinvarianten feldern, *Nuovo cimento* **22**, 1051 (1961).
- [2] S. J. Summers and R. Werner, The vacuum violates bell's inequalities, *Physics letters. A* **110**, 257 (1985).
- [3] E. Witten, Aps medal for exceptional achievement in research: Invited article on entanglement properties of quantum field theory, *Rev. Mod. Phys.* **90**, 045003 (2018).
- [4] H. Casini and M. Huerta, Entanglement entropy in free quantum field theory, *Journal of Physics A: Mathematical and Theoretical* **42**, 504007 (2009).
- [5] M. R. Vázquez, M. del Rey, H. Westman, and J. León, Local quanta, unitary inequivalence, and vacuum entanglement, *Annals of Physics* **351**, 112 (2014).
- [6] J. Keaveney, A. Sargsyan, U. Krohn, I. G. Hughes, D. Sarkisyan, and C. S. Adams, Cooperative Lamb shift in an atomic vapor layer of nanometer thickness, *Physical review letters* **108**, 173601 (2012).
- [7] R. B. Hutson, W. R. Milner, L. Yan, J. Ye, and C. Sanner, Observation of millihertz-level cooperative Lamb shifts in an optical atomic clock, *Science (American Association for the Advancement of Science)* **383**, 384 (2024).
- [8] G. T. Moore, Quantum theory of the electromagnetic field in a variable-length one-dimensional cavity, *Journal of mathematical physics* **11**, 2679 (1970).
- [9] S. A. Fulling and P. C. W. Davies, Radiation from a moving mirror in two dimensional space-time: Conformal anomaly, *Proceedings of the Royal Society of London. Series A, Mathematical and physical sciences* **348**, 393 (1976).
- [10] P. C. W. Davies and S. A. Fulling, Radiation from moving mirrors and from black holes, *Proceedings of the Royal Society of London. Series A, Mathematical and physical sciences* **356**, 237 (1977).
- [11] N. D. Birrell and P. C. W. Davies, *Quantum Fields in Curved Space*, Cambridge Monographs on Mathematical Physics (Cambridge University Press, 1982).
- [12] S. W. Hawking, Black hole explosions?, *Nature (London)* **248**, 30 (1974).
- [13] S. R. Wadia and S. W. Hawking, Particle creation by black holes, *Resonance* **26**, 133 (2021).
- [14] W. G. Unruh, Notes on black-hole evaporation, *Phys. Rev. D* **14**, 870 (1976).
- [15] L. C. B. Crispino, A. Higuchi, and G. E. A. Matsas, The unruh effect and its applications, *Rev. Mod. Phys.* **80**, 787 (2008).
- [16] D. Su, C. T. M. Ho, R. B. Mann, and T. C. Ralph, Quantum circuit model for non-inertial objects: a uniformly accelerated mirror, *New Journal of Physics* **19**, 063017 (2017).
- [17] V. Dodonov, Fifty years of the dynamical casimir effect, *Physics* **2**, 67 (2020).
- [18] T.-D. Chung and H. Verlinde, Dynamical moving mirrors and black holes, *Nuclear Physics B* **418**, 305 (1994).
- [19] C. Holzhey, F. Larsen, and F. Wilczek, Geometric and renormalized entropy in conformal field theory, *Nuclear physics b* **424**, 443 (1994).
- [20] M. R. R. Good, E. V. Linder, and F. Wilczek, Moving mirror model for quasithermal radiation fields, *Phys. Rev. D* **101**, 025012 (2020).
- [21] I. Akal, Y. Kusuki, N. Shiba, T. Takayanagi, and Z. Wei, Holographic moving mirrors, *Classical and Quantum Gravity* **38**, 224001 (2021).
- [22] V. V. Dodonov, Current status of the dynamical Casimir effect, *Physica scripta* **82**, 038105 (2010).
- [23] C. M. Wilson, G. Johansson, A. Pourkabirian, M. Simeon, J. R. Johansson, T. Duty, F. Nori, and P. Delsing, Observation of the dynamical Casimir effect in a superconducting circuit, *Nature (London)* **479**, 376 (2011).
- [24] P. Lähteenmäki, G. S. Paraoanu, J. Hassel, and P. J. Hakonen, Dynamical Casimir effect in a josephson metamaterial, *Proceedings of the National Academy of Sciences - PNAS* **110**, 4234 (2013).
- [25] E. G. Brown, M. del Rey, H. Westman, J. León, and A. Dragan, What does it mean for half of an empty cavity to be full?, *Physical Review D* **91** (2015).
- [26] M. Johanning, A. F. Varón, and C. Wunderlich, Quantum simulations with cold trapped ions, *Journal of physics. B, Atomic, molecular, and optical physics* **42**, 154009 (2009).
- [27] M. Endres, H. Bernien, A. Keesling, H. Levine, E. R. Anschuetz, A. Krajenbrink, C. Senko, V. Vuletic, M. Greiner, and M. D. Lukin, Atom-by-atom assembly of defect-free one-dimensional cold atom arrays, *Science* **354**, 1024 (2016).
- [28] F. Shah, T. L. Patti, O. Rubies-Bigorda, and S. F. Yelin, Quantum computing with subwavelength atomic arrays, *Phys. Rev. A* **109**, 012613 (2024).
- [29] A. Browaeys and T. Lahaye, Many-body physics with individually controlled rydberg atoms, *Nature physics* **16**, 132 (2020).
- [30] N. Arya and M. Zych, Selective amplification of a gravitational wave signal using an atomic array (2024), [arXiv:2408.12436 \[quant-ph\]](https://arxiv.org/abs/2408.12436).
- [31] M. A. Norcia, H. Kim, W. B. Cairncross, M. Stone, A. Ryou, M. Jaffe, M. O. Brown, K. Barnes, P. Battaglini, T. C. Bohdanowicz, A. Brown, K. Cassella, C.-A. Chen, R. Coxe, D. Crow, J. Epstein, C. Griger, E. Halperin, F. Hummel, A. M. W. Jones, J. M. Kindem, J. King, K. Kotru, J. Lauigan, M. Li, M. Lu, E. Megidish, J. Marjanovic, M. McDonald, T. Mittiga, J. A. Muniz, S. Narayanaswami, C. Nishiguchi, T. Paule, K. A. Pawlak, L. S. Peng, K. L. Pudenz, D. Rodríguez Pérez, A. Smull, D. Stack, M. Urbanek, R. J. M. van de Veerdonk, Z. Vendeiro, L. Wadleigh, T. Wilkason, T.-Y. Wu, X. Xie, E. Zalusky-Geller, X. Zhang, and B. J. Bloom, Iterative assembly of  $^{171}\text{Yb}$  atom arrays with cavity-enhanced optical lattices, *PRX Quantum* **5**, 030316 (2024).
- [32] R. Tao, M. Ammenwerth, F. Gyger, I. Bloch, and J. Zeiher, High-fidelity detection of large-scale atom arrays in an optical lattice, *Phys. Rev. Lett.* **133**, 013401 (2024).
- [33] H.-T. Zheng, X.-F. Zhou, G.-C. Guo, and Z.-W. Zhou, Enhancing analog unruh effect via superradiance in a cylindrical cavity, *Physical review research* **7**, 013027 (2025).

- [34] A. Deswal, N. Arya, K. Lochan, and S. K. Goyal, [Time-resolved and superradiantly amplified unruh signal](#) (2025), [arXiv:2501.16219 \[quant-ph\]](#).
- [35] D. Castells-Graells, J. I. Cirac, and D. S. Wild, [Cavity quantum electrodynamics with atom arrays in free space](#) (2024), [arXiv:2409.15434 \[quant-ph\]](#).
- [36] R. Bekenstein, I. Pikovski, H. Pichler, E. Shahmoon, S. F. Yelin, and M. D. Lukin, Quantum metasurfaces with atom arrays, *Nature physics* **16**, 676 (2020).
- [37] S. R. Hastings, M. J. A. de Dood, H. Kim, W. Marshall, H. S. Eisenberg, and D. Bouwmeester, Ultrafast optical response of a high-reflectivity gas al as bragg mirror, *Applied Physics Letters* **86**, 031109 (2005).
- [38] W. E. Lamb and R. C. Retherford, Fine structure of the hydrogen atom by a microwave method, *Phys. Rev.* **72**, 241 (1947).
- [39] K. Srakaew, P. Weckesser, S. Hollerith, D. Wei, D. Adler, I. Bloch, and J. Zeiher, A subwavelength atomic array switched by a single rydberg atom, *Nature physics* **19**, 714 (2023).
- [40] E. Shahmoon, D. S. Wild, M. D. Lukin, and S. F. Yelin, Co-operative resonances in light scattering from two-dimensional atomic arrays, *Physical review letters* **118**, 113601 (2017).
- [41] E. Shahmoon, M. D. Lukin, and S. F. Yelin, Quantum optomechanics of a two-dimensional atomic array, *Phys. Rev. A* **101**, 063833 (2020).
- [42] V. Dodonov and A. Klimov, Long-time asymptotics of a quantized electromagnetic field in a resonator with oscillating boundary, *Physics Letters A* **167**, 309 (1992).
- [43] V. V. Dodonov and A. B. Klimov, Generation and detection of photons in a cavity with a resonantly oscillating boundary, *Phys. Rev. A* **53**, 2664 (1996).
- [44] A. Lambrecht, M.-T. Jaekel, and S. Reynaud, Motion induced radiation from a vibrating cavity, *Phys. Rev. Lett.* **77**, 615 (1996).
- [45] E. G. Brown and J. Louko, Smooth and sharp creation of a dirichlet wall in 1+1 quantum field theory: how singular is the sharp creation limit?, *The journal of high energy physics* **2015**, 1 (2015).
- [46] J. Foo, S. Onoe, M. Zych, and T. C. Ralph, Generating multipartite entanglement from the quantum vacuum with a finite-lifetime mirror, *New Journal of Physics* **22**, 083075 (2020).
- [47] I. S. Gradshteyn and I. M. Ryzhik, [Table of integrals, series, and products](#) (Academic press, 2014).

### Appendix A: Reflective Hamiltonian Derivation

In this section, we derive the Hamiltonian for a cavity containing a reflective membrane that reflects only at a single specific frequency. In our quantum-controlled model, this will correspond to the Hamiltonian of the photonic cavity, when the atomic array is in its reflective state. We first consider the decomposition of the modes of a photonic cavity into its sub-regions, as described in Ref. [25]. The global cavity modes ( $\hat{b}_n$ ) are related to the modes of the left and right sub-cavities ( $\hat{a}_l$  for the left sub-cavity and  $\hat{a}_r$  for the right sub-cavity) through the following Bogoliubov transformation:

$$\hat{b}_n = \sum_l \alpha_{ln} \hat{a}_l - \beta_{ln} \hat{a}_l^\dagger + \bar{\alpha}_{ln} \hat{a}_l - \bar{\beta}_{ln} \hat{a}_l^\dagger. \quad (\text{A1})$$

To isolate the contribution of a specific set of modes  $\{\hat{a}_k\}$  that are reflected by the array, we subtract the terms corresponding to those modes from the global mode expression. Specifically, by subtracting the contributions of the  $\hat{a}_1$  mode (from the left sub-cavity) and the set of modes  $\hat{a}_k$ , for  $k \geq 1$  (from the right sub-cavity), we define a modified global mode  $\tilde{b}_n$  as:

$$\begin{aligned} \tilde{b}_n &= \hat{b}_n - \alpha_{1n} \hat{a}_1 + \beta_{1n} \hat{a}_1^\dagger + \sum_k -\bar{\alpha}_{kn} \hat{a}_k + \bar{\beta}_{kn} \hat{a}_k^\dagger \\ &= \sum_{l \geq 2} \alpha_{ln} \hat{a}_l - \beta_{ln} \hat{a}_l^\dagger + \sum_{l \neq k} \bar{\alpha}_{ln} \hat{a}_l - \bar{\beta}_{ln} \hat{a}_l^\dagger. \end{aligned} \quad (\text{A2})$$

This explicitly subtracts the contributions of the  $\hat{a}_1$  and  $\hat{a}_k$  modes, thereby modifying the global mode  $\hat{b}_n$  to exclude their contributions. If we now expand the global Hamiltonian in terms of each of the sub-cavity modes, and isolate out the contributions from the single frequency sub-cavity modes  $\hat{a}_1$  and  $\hat{a}_k$  (in general this represents that when the mirror is off-centre, in general a higher order modes  $k \geq 1$  can be the frequency which is filtered by the mirror), we obtain:

$$\begin{aligned} \hat{H} &= \sum_n \left[ \Omega_n \tilde{b}_n^\dagger \tilde{b}_n + \Omega_n \alpha_{1n} (\tilde{b}_n \hat{a}_1^\dagger + \hat{a}_1 \tilde{b}_n^\dagger) - \Omega_n \beta_{1n} (\hat{a}_1 \tilde{b}_n + \tilde{b}_n^\dagger \hat{a}_1^\dagger) + \Omega_n \left( (\alpha_{1n}^2 + \beta_{1n}^2) \hat{a}_1^\dagger \hat{a}_1 \right) \right. \\ &\quad \left. - \Omega_n \alpha_{1n} \beta_{1n} (\hat{a}_1^\dagger \hat{a}_1^\dagger + \hat{a}_1 \hat{a}_1) + \Omega_n \beta_{1n}^2 \right] - \sum_k \left[ \Omega_n \bar{\beta}_{kn} \left( \hat{a}_k \tilde{b}_n + \tilde{b}_n^\dagger \hat{a}_k^\dagger \right) - \Omega_n \bar{\alpha}_{kn} (\tilde{b}_n^\dagger \hat{a}_k + \hat{a}_k^\dagger \tilde{b}_n) \right. \\ &\quad \left. + \Omega_n (\alpha_{1n} \bar{\alpha}_{kn} + \bar{\beta}_{kn} \beta_{1n}) (\hat{a}_1^\dagger \hat{a}_k + \hat{a}_1 \hat{a}_k^\dagger) - \Omega_n (\alpha_{1n} \bar{\beta}_{kn} + \bar{\alpha}_{kn} \beta_{1n}) (\hat{a}_1^\dagger \hat{a}_k^\dagger + \hat{a}_1 \hat{a}_k) \right. \\ &\quad \left. + \Omega_n \left( (\bar{\alpha}_{kn}^2 + \bar{\beta}_{kn}^2) \hat{a}_k^\dagger \hat{a}_k \right) - \Omega_n \bar{\alpha}_{kn} \bar{\beta}_{kn} \left( \hat{a}_k^\dagger \hat{a}_k^\dagger + \hat{a}_k \hat{a}_k \right) + \Omega_n \bar{\beta}_{kn}^2 \right]. \end{aligned} \quad (\text{A3})$$

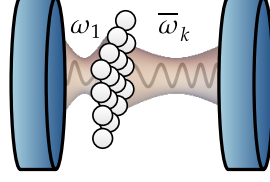


FIG. 4: An atom array in a photonic cavity that is highly reflective within some frequency band-width  $\Delta$ , can trap standing waves of frequency  $\omega_1 \in \Delta$  of the left sub-cavity, and  $\bar{\omega}_k \in \Delta$  of the right sub-cavity. The Hamiltonian for an atom array that is highly reflective in this frequency band-width can be constructed as the sum of free Hamiltonian terms of the left and right sub-cavities, including vacuum terms.

The presence of the single frequency mirror removes the interactions between the  $\hat{a}_1$  mode and all right sub-cavity modes, as well as all  $\hat{a}_k$  modes and all left sub-cavity modes. This follows how for the perfectly reflecting mirror considered in Sec. II, the effect of the mirror is to remove interactions and squeezing terms across the sub-cavity modes that are present in the global cavity Hamiltonian. Applying the same principle, but restricted to the set of frequencies reflected by the array, we obtain,

$$\begin{aligned} \hat{H} &= \omega_1 \hat{a}_1^\dagger \hat{a}_1 + \sum_n \left[ \Omega_n \tilde{b}_n^\dagger \tilde{b}_n + \Omega_n \beta_{1n}^2 \right] + \sum_k \left[ \bar{\omega}_k \hat{a}_k^\dagger \hat{a}_k \right] + \sum_{k,n} \left[ \Omega_n \bar{\beta}_{kn}^2 \right], \\ &\approx \omega_1 \hat{a}_1^\dagger \hat{a}_1 + \sum_n \Omega_n \tilde{b}_n^\dagger \tilde{b}_n + \sum_k \bar{\omega}_k \hat{a}_k^\dagger \hat{a}_k, \end{aligned} \quad (\text{A4})$$

where the sum over  $k$  extends to all right sub-cavity modes that the single frequency mirror reflects (all modes that fall within the linewidth of the atomic array's reflectivity), and in the second line we have taken the limit  $L \gg r$ , where  $r$  is the size of the sub-cavity, and neglected all other terms as they are sub-leading in this regime. In this regime, the dominant frequency shift between the transmissive and reflective states comes from difference in particle content, rather than constant offsets  $\Omega_n \beta_{1n}^2, \Omega_n \bar{\beta}_{kn}^2$ . The Hamiltonian of Eq. (A4) represents standing waves at the frequency  $\omega_1$  in the left sub-cavity, with standing waves of frequencies being one of the  $\bar{\omega}_k$  frequencies in the right sub-cavity as displayed in Fig. 4.

We now construct the Hamiltonian of the global cavity with the sub-cavities removed as

$$\hat{H}_\perp = \sum_n \Omega_n \tilde{b}_n^\dagger \tilde{b}_n, \quad (\text{A5})$$

which is completely orthogonal to the individual single frequency sub-cavities as

$$[\hat{H}_\perp, \omega_1 \hat{a}_1^\dagger \hat{a}_1] = [\hat{H}_\perp, \bar{\omega}_1 \hat{a}_1^\dagger \hat{a}_1] = 0. \quad (\text{A6})$$

We therefore, use the following Hamiltonian for the single frequency reflective mirror in the  $L \gg r$  regime,

$$\hat{H}_R = \omega_1 \hat{a}_1^\dagger \hat{a}_1 + \sum_n \Omega_n \tilde{b}_n^\dagger \tilde{b}_n + \sum_k \bar{\omega}_k \hat{a}_k^\dagger \hat{a}_k, \quad (\text{A7})$$

noting that the commutator

$$\begin{aligned} [\tilde{b}_i, \tilde{b}_j^\dagger] &= \delta_{ij} + \alpha_{1i} \alpha_{1j}^* - \beta_{1i} \beta_{1j}^* + \sum_k \bar{\alpha}_{ki} \bar{\alpha}_{kj}^* - \bar{\beta}_{ki} \bar{\beta}_{kj}^*, \\ &= \delta_{ij} + \frac{\sqrt{ij}(-1)^{i+j} \sin(i\pi a) \sin(j\pi a)}{\pi^2 (aj-1)(ai-1)} - \frac{\sqrt{ij}(-1)^{i+j} \sin(i\pi a) \sin(j\pi a)}{\pi^2 (aj+1)(ai+1)} \\ &\quad + \frac{k \sin(i\pi a) \sin(j\pi a)}{\sqrt{ij} \pi^2 (\bar{a}'j-k)(\bar{a}'i-k)} - \frac{k \sin(i\pi a) \sin(j\pi a)}{\sqrt{ij} \pi^2 (\bar{a}'j+k)(\bar{a}'i+k)} \end{aligned} \quad (\text{A8})$$

in the regime  $L \gg r$ , the commutator approaches  $[\tilde{b}_i, \tilde{b}_j^\dagger] = \delta_{ij} + O(a^2)$ , and we obtain a division of the sub-cavities in terms of purely orthogonal modes in this limit.



## Appendix B: Perturbative dynamics of a Quantum-Controlled Photonic Cavity

Here we present a perturbative analytical solution of the dynamics of a quantum-controlled photonic cavity. To derive this, we consider the full Hamiltonian, including the free Hamiltonian of the control:

$$\hat{H} = \frac{\hbar\nu}{2}(|R\rangle\langle R| - |T\rangle\langle T|) + \hat{H}_T \otimes |T\rangle\langle T| + \hat{H}_R \otimes |R\rangle\langle R| + g(|T\rangle\langle R| e^{+i\omega_D t} + |R\rangle\langle T| e^{-i\omega_D t}), \quad (\text{B1})$$

which includes a drive on the qubit of strength  $g$  and frequency  $\omega_D$ . Now transforming to the rotating frame of the control, produces:

$$\hat{H} \rightarrow e^{i\hat{H}_{\text{free}}t/\hbar} \hat{H} e^{-i\hat{H}_{\text{free}}t/\hbar} = \hat{H}_T \otimes |T\rangle\langle T| + \hat{H}_R \otimes |R\rangle\langle R| + g(|T\rangle\langle R| e^{i(\omega_D - \nu)t} + |R\rangle\langle T| e^{i(\nu - \omega_D)t}), \quad (\text{B2})$$

where  $\hat{H}_{\text{free}} = (\hbar\nu/2)(|R\rangle\langle R| - |T\rangle\langle T|)$  is the free Hamiltonian of the control. We now break up the following contributions to the Hamiltonian:

$$\begin{aligned} \hat{H}_0 &= \hat{H}_T \otimes |T\rangle\langle T| + \hat{H}_R \otimes |R\rangle\langle R| \\ \hat{H}_g &= g(|T\rangle\langle R| e^{i(\omega_D - \nu)t} + |R\rangle\langle T| e^{-i(\omega_D - \nu)t}). \end{aligned} \quad (\text{B3})$$

We treat  $\hat{H}_g$  as a perturbation, and work in the interaction picture:

$$\hat{H}_g(t) = e^{i\hat{H}_0 t} \hat{H}_g e^{-i\hat{H}_0 t}. \quad (\text{B4})$$

we have  $|\psi(t)\rangle_I = e^{i\hat{H}_0 t} |\psi(t)\rangle_S = U_I(t) |\psi_I(0)\rangle$ , where

$$U_I(t) = \mathcal{T} \left\{ e^{-i \int_0^t dt' \hat{H}_g(t')} \right\} = \hat{\mathbb{I}} - i \int_0^t dt' \hat{H}_g(t') - \frac{1}{2} \int_0^t dt' \int_0^{t'} dt'' \hat{H}_g(t') \hat{H}_g(t'') + \dots, \quad (\text{B5})$$

where  $\mathcal{T}$  denotes time-ordering. Including terms up to second order in  $g$ , gives explicitly

$$\begin{aligned} \hat{U}_I^{(2)} &= \hat{\mathbb{I}} - ig \int_0^t dt' (e^{i\hat{H}_T t'} |T\rangle\langle R| e^{-i\hat{H}_R t'} e^{i(\omega_D - \nu)t'} + \text{h.c.}) \\ &\quad - \frac{g^2}{2} \int_0^t dt' \int_0^{t'} dt'' (e^{i\hat{H}_T t'} |T\rangle\langle R| e^{-i\hat{H}_R t'} e^{i(\omega_D - \nu)t'} + \text{h.c.}) (e^{i\hat{H}_T t''} |T\rangle\langle R| e^{-i\hat{H}_R t''} e^{i(\omega_D - \nu)t''} + \text{h.c.}) + O(g^2) \\ &= \hat{\mathbb{I}} - ig \int_0^t dt' (e^{i\hat{H}_T t'} |T\rangle\langle R| e^{-i\hat{H}_R t'} e^{i(\omega_D - \nu)t'} + \text{h.c.}) \\ &\quad - \frac{g^2}{2} \int_0^t dt' \int_0^{t''} dt'' (e^{i\hat{H}_T t'} |T\rangle\langle R| e^{-i\hat{H}_R t'} e^{i\hat{H}_T t''} |T\rangle\langle R| e^{-i\hat{H}_R t''} e^{i(\omega_D - \nu)(t' + t'')}) \\ &\quad + e^{i\hat{H}_T t'} |T\rangle\langle R| e^{-i\hat{H}_R t'} e^{i\hat{H}_R t''} |R\rangle\langle T| e^{-i\hat{H}_T t''} e^{i(\omega_D - \nu)(t' - t'')} \\ &\quad + e^{i\hat{H}_R t'} |R\rangle\langle T| e^{-i\hat{H}_T t'} e^{i\hat{H}_T t''} |T\rangle\langle R| e^{-i\hat{H}_R t''} e^{-i(\omega_D - \nu)(t' - t'')} \\ &\quad + e^{i\hat{H}_R t'} |R\rangle\langle T| e^{-i\hat{H}_T t'} e^{i\hat{H}_R t''} |R\rangle\langle T| e^{i\hat{H}_T t''} e^{-i(\omega_D - \nu)(t' + t'')} + O(g^3). \end{aligned} \quad (\text{B6})$$

In the main text, this unitary is restricted to  $O(g)$  terms relevant for the leading order computations of the transition rate of the control atom. If the control is initially in the transmissive state, the probability for it to flip to the reflective state after unitary evolution up to  $O(g)$  is

$$P_R = g^2 \int_0^t dt' dt'' \langle 0_T | e^{i\hat{H}_R(t' - t'')} | 0_T \rangle e^{i(\omega_D - \nu)(t' - t'')}, \quad (\text{B7})$$

which is used in the main text.

### Appendix C: Analytical Estimate for the Frequency shift

In this section, we derive the analytical estimate for the frequency shift in the control due to particle-creation from the vacuum. The full Hamiltonian, in the rotating frame of the control atom is

$$\hat{H} = \hat{H}_{\text{cav}} + \hat{H}_{\text{switch}}, \quad (\text{C1})$$

where,

$$\begin{aligned} \hat{H}_{\text{cav}} &= \hat{H}_T \otimes |T\rangle\langle T| + \hat{H}_R \otimes |R\rangle\langle R| \\ \hat{H}_{\text{switch}} &= g \left( |T\rangle\langle R| e^{i(\omega_D - \nu)t} + \text{h.c.} \right), \end{aligned} \quad (\text{C2})$$

here  $\hat{H}_T = \sum_n \Omega_n \hat{b}_n^\dagger \hat{b}_n$  and  $\hat{H}_R = \omega_1 \hat{a}_1^\dagger \hat{a}_1 + \sum_n \Omega_n \tilde{b}_n^\dagger \tilde{b}_n + \sum_k \bar{\omega}_k \hat{a}_k^\dagger \hat{a}_k$ . Now, we can express  $\hat{a}_1^\dagger \hat{a}_1$  in terms of the global modes as

$$\omega_1 \hat{a}_1^\dagger \hat{a}_1 = \sum_n \left( \omega_n \hat{b}_n^\dagger \hat{b}_n - g_n \hat{b}_n^\dagger \hat{b}_n^\dagger - g_n^* \hat{b}_n \hat{b}_n \right) + \sum_{n \neq m} \left( f_{n,m} \hat{b}_n^\dagger \hat{b}_m - g_{n,m} \hat{b}_n^\dagger \hat{b}_m^\dagger - g_{m,n}^* \hat{b}_n \hat{b}_m + f_{n,m}^* \hat{b}_n \hat{b}_m^\dagger \right). \quad (\text{C3})$$

where,

$$\begin{aligned} \omega_n &= \omega_1 \left( |\alpha_{1,n}|^2 + |\beta_{1,n}|^2 \right), \\ f_{n,m} &= \omega_1 \alpha_{1,n} \alpha_{1,m}^*, \\ g_n &= \omega_1 \alpha_{1,n} \beta_{1,n}^*, \\ g_{n,m} &= \omega_1 \alpha_{1,n} \beta_{1,m}^*. \end{aligned} \quad (\text{C4})$$

Now, if we convert into the rotating frame of  $\hat{H}_T \otimes |R\rangle\langle R|$ , we can drop all of the counter-rotating terms, and then when converting back out of the rotating frame, we will be left with the  $\sum_n \omega_n \hat{b}_n^\dagger \hat{b}_n$  term. This will produce the Hamiltonian:

$$\hat{H}_{\text{cav}} = \hat{H}_T \otimes |T\rangle\langle T| + \left( \sum_n \left( \omega_n \hat{b}_n^\dagger \hat{b}_n + \Omega_n \hat{b}_n^\dagger \hat{b}_n + \Omega_n \tilde{b}_n^\dagger \tilde{b}_n + \omega_1 |\beta_{1,n}|^2 \right) + \sum_k \bar{\omega}_k \hat{a}_k^\dagger \hat{a}_k \right) \otimes |R\rangle\langle R|, \quad (\text{C5})$$

then as derived previously, after conversion to the interaction picture,

$$P_R = g^2 \int_0^t dt' dt'' \langle 0_T | e^{i\hat{H}_R(t'-t'')} | 0_T \rangle e^{i(\omega_D - \nu)(t'-t'')}, \quad (\text{C6})$$

gives the probability for the control atom to transition. The analytical estimate for the frequency shift

$$\delta_R = \sum_n \omega_1 |\beta_{1,n}|^2, \quad (\text{C7})$$

provides a good approximation of the precise numerical solution. We have omitted the contribution from the  $\sum_n \tilde{b}_n^\dagger \tilde{b}_n$  term in the Hamiltonian derived in Appendix A, as we numerically evaluate their contribution to be sub-leading to  $\mathcal{O}(10^{-6})$ , while the dominant contribution to the frequency shift evaluates to be  $\sum_n |\beta_{1,n}|^2 \approx 0.075$ . This is the frequency shift which we use in the main text. We have further omitted the contribution from the  $\sum_k \bar{\omega}_k \hat{a}_k^\dagger \hat{a}_k$  term as this provides a negligible contribution in the regime  $L \gg r$ .

### Appendix D: Imperfect Reflectivity

Our toy model for a mirror with imperfect reflectivity is adapted from Ref. [45], which considers particle content due to the presence of a time-dependent boundary condition at the origin of Minkowski spacetime, as well as that of a cavity with

boundaries at  $x = \pm a/2$ . A similar problem was considered in Ref. [46], for a mirror following conformal diamond time with tunable reflectivity.

We consider a real massless scalar field  $\hat{\phi} \equiv \hat{\phi}(t, x)$ . Introducing a mirror at  $x = 0$  modifies the scalar Klein-Gordon equation to read,

$$\partial_t^2 \hat{\phi} - \Delta_{\theta(t)} \hat{\phi} = 0 \quad (\text{D1})$$

where  $\{-\Delta_{\theta} | \theta \in [0, \pi/2]\}$  is the one-parameter family of self-adjoint extensions of  $-\partial_x^2$  on  $L^2(\mathbb{R} \setminus \{0\})$ . The limiting cases  $\theta(t) = 0, \pi/2$  correspond to a perfectly reflective and transmissive boundary respectively, with intermediate values interpolating between the two. One can write Eq. (D1) as,

$$\left[ \partial_t^2 - \partial_x^2 + \frac{2 \cot(\theta(t))}{L} \delta(x) \right] \hat{\phi} = 0 \quad (\text{D2})$$

where  $L$  has dimensions of length, which we henceforth set to unity. The presence of the mirror thus acts as a potential term proportional to  $\delta(x)$  with a time-dependent coefficient, tending to zero as  $\theta \rightarrow (\pi/2)_-$  and to  $+\infty$  as  $\theta \rightarrow 0_+$ . Assuming without loss of generality that the mirror switching begins at  $t = 0$ , we may parametrise  $\theta(t)$  as,

$$\theta(t) = \begin{cases} \pi/2 & t \leq 0 \\ \cot^{-1}(\lambda \cot(h(\lambda t))) & 0 < t < \lambda^{-1} \\ 0 & t \geq \lambda^{-1} \end{cases} \quad (\text{D3})$$

i.e. the mirror becomes perfect reflective at  $t = \lambda^{-1}$ .  $h(y)$  is a smooth function such that  $h(y) = \pi/2$  for  $y \leq 0$ ,  $0 < h(y) < \pi/2$  for  $0 < y < 1$  and  $h(y) = 0$  for  $y \geq 1$ . Taking  $h(y) = \tan^{-1}(1 + e^{-y})$ , one obtains

$$\theta(t) = \tan^{-1} \left( \frac{1 + e^{-\lambda t}}{\lambda} \right) \quad (\text{D4})$$

as discussed in the main text. To obtain the mode functions with frequency  $k$ , we make the ansatz,

$$U_k(u, v) = \frac{1}{\sqrt{8\pi k}} \left[ e^{-ikv} + E_k(u) \right] \quad (\text{D5})$$

where  $v = t + x, u = t - x$  are lightcone coordinates and  $E_k(u)$  is to be found. Note that the spatially odd solutions to the field equation Eq. (D1) do not feel the presence of the wall; only the spatially even solutions do. By spatial evenness, it suffices to consider these solutions in the half-space  $x > 0$ , where those in the space  $x < 0$  follow by the replacement  $(t, x) \rightarrow (t, -x)$ . If we restrict ourselves, for simplicity, to the right-moving modes, then it can be shown that the constraints imposed by Eq. (D2) and (D3) imply solutions of the form,

$$E_k(u) = R_{k/\lambda}(\lambda u) \quad (\text{D6})$$

where

$$R_K(y) = \begin{cases} e^{-iKy} & y \leq 0 \\ e^{-iKy} - \frac{2}{B(y)} \int_0^y B'(y') e^{-iKy'} dy' & 0 < y < 1 \\ -e^{-iKy} & y \geq 1 \end{cases} \quad (\text{D7})$$

and  $B(y)$  is a solution to  $B'(y)/B(y) = \cot(h(y))$  with the initial condition  $B(0) = 1$ . For the choice of  $h(y)$  given above, the right-moving modes during the switching are given by [45]

$$\bar{U}_k(u) = \frac{1}{\sqrt{8\pi k}} \frac{e^{-iku}}{1 + e^{\lambda u}} \left( 1 - \frac{\lambda + ik}{\lambda - ik} e^{\lambda u} \right). \quad (\text{D8})$$

Henceforth, we work with the cavity modes explicitly, which can be obtained from Eq. (D8) by replacing the prefactor  $(8\pi k)^{-1/2}$  with  $(4\pi m)^{-1/2}$  where  $m \in \mathbb{Z}$  and restricting  $k = \pi m/a$ . Meanwhile, the standing wave solutions of the global cavity are simply  $U_m(u) = (4\pi m)^{-1/2} e^{-i\pi m u/a}$ . We can expand the subcavity mode operators  $\hat{a}_m$  in a basis of the global mode operators  $(\hat{b}_n, \hat{b}_n^\dagger)$  via the Bogoliubov transformation,

$$\hat{a}_m = \sum_{n=1}^{+\infty} \left( \alpha_{nm} \hat{b}_n + \beta_{nm} \hat{b}_n^\dagger \right) \quad (\text{D9})$$

where the Bogoliubov coefficients  $\alpha_{nm}, \beta_{nm}$  are defined in the usual way via the Klein-Gordon inner product. In the vacuum of the unperturbed modes, the expectation value of the particle number of the new modes is,

$$\langle 0_B | \hat{a}_m^\dagger \hat{a}_m | 0_B \rangle = \sum_{n=1}^{+\infty} |\beta_{nm}|^2 \quad (\text{D10})$$

It now remains to compute the Bogoliubov coefficients  $\beta_{k\omega}$ , which are given by

$$\beta_{nm} = \langle U_m^*(u), \bar{U}_n(u) \rangle = i \int_0^{a/2} du \left( U_m(u) \partial_u \bar{U}_n - \bar{U}_n \partial_u U_m \right) \quad (\text{D11})$$

Upon integration, one obtains,

$$\begin{aligned} \beta_{nm} = & \frac{1}{4\pi} \sqrt{\frac{n}{m}} \left( \frac{ie^{-ia\vartheta\lambda}}{\vartheta\lambda} {}_2F_1\left(1 - i\vartheta, 1 - i\vartheta, -e^{a\lambda/2}\right) + \frac{1}{2\lambda} \left( \psi^{(0)}(-i\vartheta/2) - \psi^{(0)}(-i\vartheta/2 + 1/2) \right) \right) \\ & - \frac{1}{4\pi} \sqrt{\frac{n}{m}} \frac{\lambda + i\pi m/a}{\lambda - i\pi m/a} \left( \frac{i}{2\vartheta\lambda} \left( 2\text{Re} \left[ e^{ia\vartheta\lambda} {}_2F_1\left(1, -i\vartheta, -i\vartheta + 1, -e^{a\lambda/2}\right) \right] - \pi\vartheta \text{csch}(\pi\theta) - 1 \right) \right. \\ & \left. + \frac{1}{2\theta\lambda} \left( 2\text{Re} \left[ ie^{-ia\vartheta\lambda} {}_2F_1\left(1, i\vartheta, i\vartheta + 1, -e^{-a\lambda/2}\right) \right] - \vartheta \text{Re} \left[ \psi^{(0)}(-i\vartheta/2) - \psi^{(0)}(-i\vartheta/2 + 1/2) \right] \right) \right) \end{aligned} \quad (\text{D12})$$

where  ${}_2F_1(\alpha, \beta, \gamma, z)$  is the hypergeometric function,  $\psi^{(0)}(z)$  is the PolyGamma function [47], and we defined  $\vartheta = (m + n)\pi/(a\lambda)$ . Substituting Eq. (D12) into Eq. (D10) gives the average particle number  $\langle \hat{N} \rangle$  in Fig. 3(b) of the main text.

### Appendix E: Non-Perturbative Transition Calculations and Cavity Intensity

If the control atom is driven off-resonance, there should be a substantially reduced probability for the control atom to flip to its reflective state. To illustrate this, we simulate the dynamics of the control atom in Fig. 5 for various coupling strengths between the control atom and the driving laser, but for a drive resonant with the un-renormalised transition frequency  $\omega_D = \nu$ . As expected for weak couplings such that  $g \ll \nu \sim \omega_1$ , the standard off-resonant suppression expected in the quantum optical Rabi model is observed, scaling as  $g^2$ .

This implies for the cavity extraction protocol, that when the cavity is driven on-resonance with the sub-cavity frequency  $\omega_1$ , that the average intensity observed in the cavity, will be suppressed by the non-zero probability for the atom array to be in the reflective state  $|c_R\rangle^2$ . The intensity of light in the cavity close to the sub-cavity frequency is

$$I = \frac{I_{\max} |c_R|^2}{1 + (2\mathcal{F}/\pi)^2 \sin^2(\pi\nu/\omega_1)}, \quad (\text{E1})$$

where  $I_{\max} = \frac{I_0}{(1-r)^2}$ ,  $\mathcal{F}$  is the finesse of the cavity,  $r$  is the optical attenuation factor due to any imperfect reflectivity of the array and  $\nu$  is the frequency of the pump. In this way, a substantial average power will only be observed in the cavity at the sub-cavity frequency, if the control atom was driven at the re-normalised frequency due to the presence of photons from entangled sub-regions of the vacuum of the global cavity.

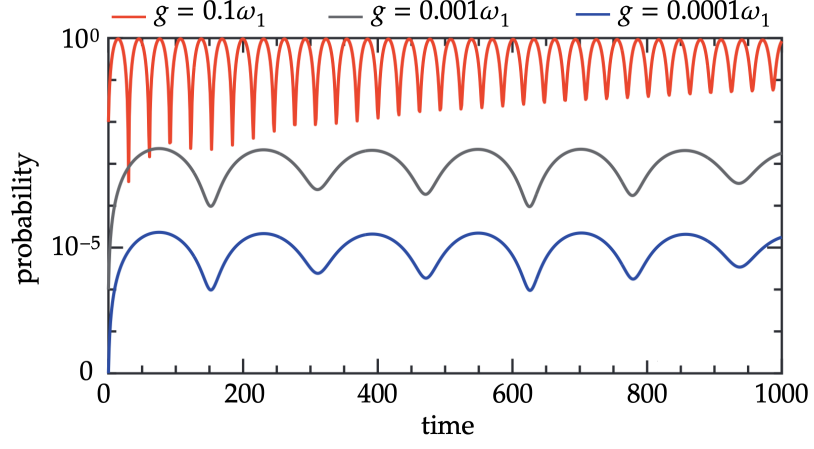


FIG. 5: Numerical solution for the probability for the control atom to flip  $P_R$  for drive resonant with the un-renormalised transition frequency  $\omega_D = \nu$ . The expected  $\mathcal{O}(g^2)$  reduction in amplitude for reduced coupling strengths is observed.